Plasma plume circulation and impact in an MHD substorm

T. E. Moore,[1] M.-C. Fok,[1] D. C. Delcourt,[2] S. P. Slinker,[3] and J. A. Fedder[4]

Received 21 January 2008; revised 14 March 2008; accepted 9 April 2008; published 20 June 2008.

[1] We investigate the fate of a plasmaspheric plume generated by a discrete period of southward interplanetary magnetic field (IMF) to assess its contribution to plasma sheet and ring current pressure and compare with that for other sources. We use test particle motions in Lyon-Fedder-Mobarry (LFM) global circulation model fields. The inner magnetosphere is simulated with the Comprehensive Ring Current Model (CRCM) model of Fok and Wolf, driven by the transpolar potential developed by the LFM magnetosphere. A variant of the Ober plasmasphere model is embedded within the models and driven by them. Global circulation is stimulated by a period of southward IMF embedded within a long interval of northward IMF. This leads to the production of a well-defined plasmaspheric plume, enhancing the plasma density sunward of the plasmasphere. Test particles are launched with the properties of plasmaspheric ions on the $L = 6.6\ R_E$ shell and weighted with densities as specified by the Ober model, as it responds to convection imposed by CRCM. Particles are tracked until they are lost from the system downstream or into the atmosphere, using the Delcourt full equations of motion, implemented for finite element fields. Results are compared with earlier computations of polar and auroral wind outflows. The plume produces an enhanced flow of plasma $\sim$10 times the normal polar wind global fluence. However, we find that most of the "plasmaspheric wind" is lost from the magnetosphere such that its contribution to the ring current energy density is comparable to that of the normal polar wind for this type of event.

Citation: Moore, T. E., M.-C. Fok, D. C. Delcourt, S. P. Slinker, and J. A. Fedder (2008), Plasma plume circulation and impact in an MHD substorm, *J. Geophys. Res.*, *113*, A06219, doi:10.1029/2008JA013050.

1. Introduction

[2] Observations have increasingly revealed that enhanced magnetospheric circulation, driven by the solar wind and its linked interplanetary magnetic field, results in the transport of the outer layers of the plasmasphere toward the dayside subsolar magnetopause, creating "plasmaspheric plumes" [*Grebowsky*, 1970; *Chappell et al.*, 1970, 1971; *Freeman et al.*, 1977; *Sandel et al.*, 2001; *Goldstein et al.*, 2004; *Chandler and Moore*, 2003; *Chen and Moore*, 2004, 2006]. The plasmasphere is supplied by a light ion outflow analogous to the polar wind, commonly known as "refilling flows" because they flow on closed low-latitude flux tubes and build up substantial densities over several days. The density of cold light ion plasmas at the magnetopause is especially enhanced during severe compressions of the magnetosphere by high solar wind pressure periods [*Su et al.*, 2001a, 2001b], and it has been suggested that this plasma may be transported through the boundary layers to the plasma sheet [*Elphic et al.*, 1997; *Borovsky et al.*, 1997; *Borovsky and Denton*, 2006] and alter the loading on reconnection or other processes. This hypothesis seems natural in view of the known circulation patterns of magnetospheric plasmas, which will certainly tend to redistribute the outer plasmaspheric material to the magnetotail via either the high-latitude or low-latitude boundary layers, depending on the orientation of the interplanetary magnetic field (IMF). By analogy to "polar wind" and "auroral wind," we refer to the episodic circulation of plasmaspheric plume material beyond the plasmasphere as "plasmaspheric wind."

[3] One of the puzzles that has come out of earlier work has been a failure to identify a denser version of the polar wind that might be expected to be associated with periods of plume generation and delivery to the dayside magnetopause region. *Borovsky et al.* [1997] and coworkers have made such searches using various sources of data, but have never found a clear "smoking gun" of plasma flow that is traceable to a plasmaspheric plume. In the ionosphere proper, there does seem to be such an extended plume, which has been traced through the polar cap region by *Foster et al.* [2004]. In view of this latter observation, it is indeed puzzling why no clear enhancement of the polar wind has been found to date.

[4] The purpose of the present work is to quantitatively assess the above hypothesis by means of theoretical simulations. We use a model of the plasmasphere that is known to be able to produce reasonable quantitative transport and resultant spatial distributions of plasmaspheric material

[1]NASA Goddard Space Flight Center, Greenbelt, Maryland, USA.
[2]Centre d'Études des l'Environnements Terrestre et Planétaires, UMR 8639, St. Maur, France.
[3]Naval Research Laboratory, Washington, D. C., USA.
[4]Icarus Research, Bethesda, Maryland, USA.

Copyright 2008 by the American Geophysical Union.
0148-0227/08/2008JA013050

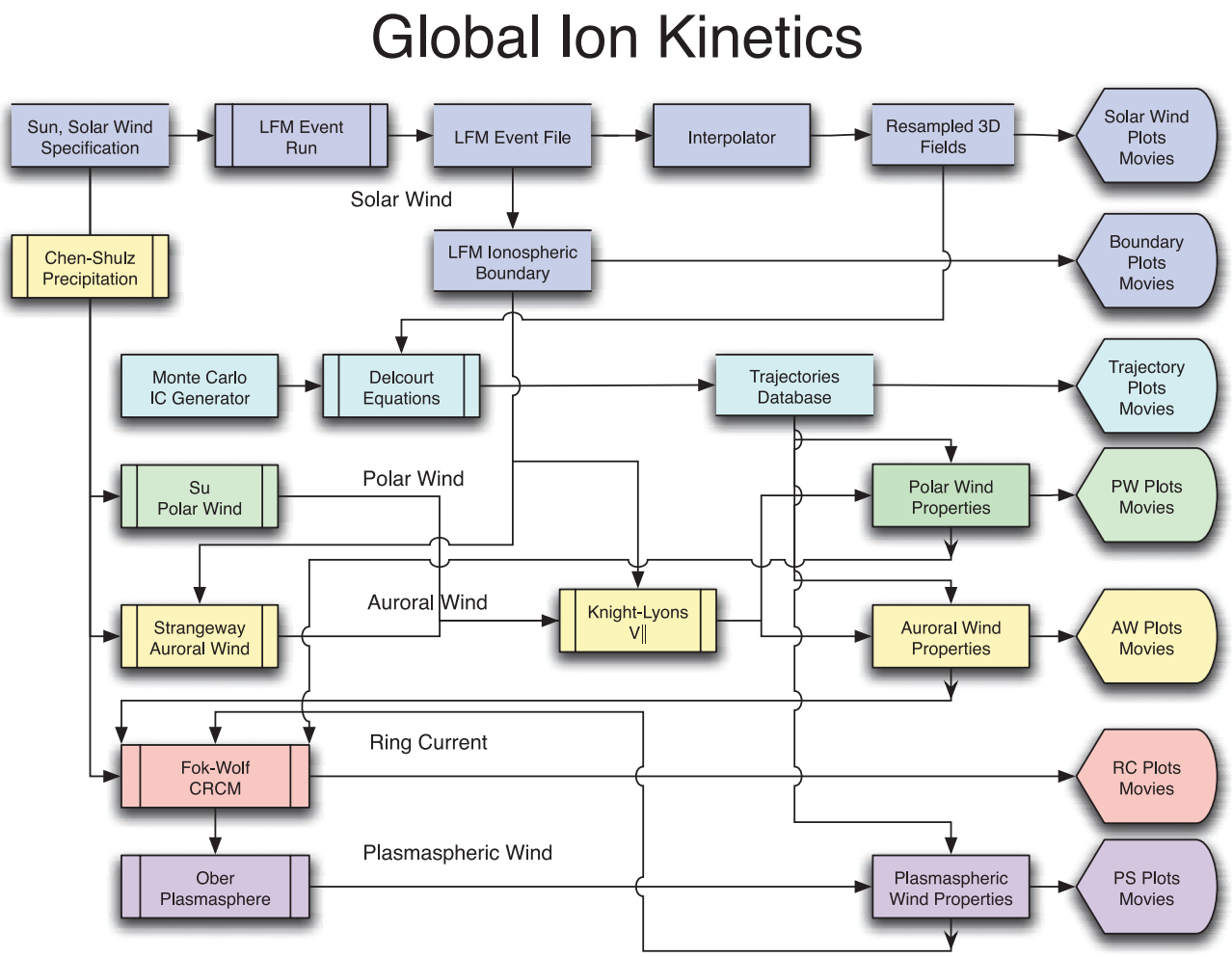

Figure 1. A flowchart of the simulation process showing the major modules and the overall flow of information between models. The flow is generally from the upper left to the lower right both overall and for each specific module. Process modules with "sidebars" are based on published work, while those without were developed by the authors for this effort.

[*Ober et al.*, 1997]. The Comprehensive Ring Current Model of *Fok et al.* [2001] drives the plasmaspheric model. It, in turn, is embedded within the global magnetospheric simulation of Lyon, Fedder, and Mobarry [*Lyon et al.*, 2004]. These models allow plasmaspheric proton test particle trajectories to be initiated at the "surface" of the plasmasphere, taken to be a magnetic shell of radius 6.6 R_E. They also support the calculation of large numbers (millions) of such trajectories, and tracking of them throughout the magnetosphere. This permits the computation of both kinetic and bulk characteristics of the ionospheric plasmas throughout the entire magnetosphere, subject only to statistical uncertainties based on the number of trajectories that are accumulated.

2. Model Descriptions

[5] Figure 1 summarizes our simulation approach. The Lyon-Fedder-Mobarry (LFM) ideal MHD global circulation model [*Lyon et al.*, 2004] provides the framework for computing ion trajectories in specified electromagnetic fields throughout the outer magnetosphere, including the magnetosheath, bow shock and beyond. Gravity is also included since the lowest-energy ions are affected. The LFM simulation tracks only a solar wind plasma fluid, with the inner boundary assumed to be magnetically coupled to an ionosphere of specified conductivity. In this work, particular attention was given to the computed hot plasma fluid parameters, electromagnetic fields, and linking current density on an inner boundary of the simulation space, because these were used to drive ionospheric outflow responses.

[6] The ionospheric conductance consisted of a component due to solar illumination and a component calculated from auroral precipitation [*Slinker et al.*, 1999]. Equinox conditions were assumed and the peak dayside conductance was about 10 mho. The dimensions of the LFM simulation space extended from +24 to −300 R_E in XSM and ±90 R_E

in YSM and ZSM. The inner boundary of the LFM simulation was at 3.2 R_E radius. The particle simulation space ranged from +24 to −70 R_E in X_{GSM}, and from ±30 R_E in Y_{GSM} and Z_{GSM}.

[7] To control and isolate the effects of solar wind variations, we elected to use a run of about 3.5 h duration, in which solar wind properties were held constant (at typical values) with the exception of the interplanetary magnetic field (IMF). The IMF was initially northward at 5 nT intensity, until about 5 min into the run, was then abruptly turned southward for two hours until 125 min, and then was returned abruptly northward for the remainder of the simulation period. The timing of the field changes will be indicated on plots below. During the sequence, a substorm-like event occurs as a result of a burst of midtail reconnection that ejects a plasmoid down the tail and produces near-Earth plasma sheet dipolarization and transport.

[8] Into this context is embedded the Comprehensive Ring Current Model [*Fok et al.*, 2001], which includes a nested plasmasphere model adapted from that of *Ober et al.* [1997]. The Comprehensive Ring Current Model (CRCM) solves the bounce averaged Vlasov equation for inner magnetospheric convection self consistently with electrodynamic coupling to the ionosphere, driven by boundary conditions derived from the LFM simulation for transpolar potential. CRCM requires that flux tubes are supplied from outside the simulation space with specified plasma content and magnetic geometry. When flux tubes convect into the space according to the imposed external convection specification, they begin to fill owing to ionospheric proton outflows that are computed so as to shut down realistically as the flux tubes fill up. The result is that flux tubes that persist inside the model space become filled within an appropriate time constant that is set by the volume of the flux tube and the assumed strength of the ionospheric outflow flux. The maximum outflow flux is essentially that of the polar wind on an empty flux tube.

[9] Using this model of the density distribution in the plasmasphere, we evaluated the plasma density on the surface defined by magnetic field lines with equatorial crossing radii at 6.6 R_E. The resultant densities were used to weight the trajectories of protons launched from this same surface, with initial velocities representative of plasmaspheric populations. The proton start points were randomly distributed in latitude and local time around this shell boundary. Their initial velocities were randomly selected from a range matching observed outer plasmasphere ion temperatures, i.e., 1 eV. Their initial pitch angles were selected randomly from the full range from 0 to 180°. Finally, their initial gyrophases were selected randomly from the full range of 360 deg. around the local convection flow speed, as specified by the global simulation, and the trajectories were computed and recorded in a database until the particles either entered the atmosphere or escaped from the simulation space, using the full equations of motion and a computation process described by, *Delcourt et al.* [1993] or *Peroomian et al.* [2007].

[10] The approach we have described above invokes a plasmasphere that is driven by the convection imposed upon the inner magnetosphere by the solar wind interaction, with flow loading attributed to the ionospheric drag via field aligned currents. It includes corotation and produces typical plasmaspheric plumes when magnetospheric convection is enhanced. We make a transition to single particle motions outside the plasmasphere proper and beyond the CRCM boundary, so that we can then track plasmaspheric plumes through the structured and variable fields of the outer magnetosphere, its boundary layers, and account for the full nonadiabatic behavior of the particles, using a suitable model of those structured fields. As a reasonable approximation of the fields, we use the ideal MHD global simulation. However, it must be noted that this approach does not allow the global simulation to react to the presence of plasmaspheric plasmas, because the plasmasphere has been treated as test parcels of plasma and the protons have been treated as test particles. On the other hand, the CRCM does compute self-consistent convection electric fields within its domain, including current flows linking the ionospheric F region. These fields do respond to the presence or absence of plasma as determined by the boundary conditions.

[11] We have previously reported the behavior of solar wind, polar wind, and auroral wind plasmas in this same MHD simulation [*Moore et al.*, 2007], as well as their contribution to the ring current for this event [*Fok et al.*, 2006]. We consider the polar wind protons to flow everywhere outside the plasmapause. We treat the auroral wind as an O^+ outflow that is embedded within the polar wind, and we accelerate both polar wind and auroral wind ions according to parallel potential drops derived from the Knight-Lyons relationship and driven by the intensity of upward coupling currents imposed by the LFM simulation at the ionospheric boundary. Further details on this treatment can be found in the cited papers.

[12] In the present work we add to this the "plasmaspheric" wind of protons from the plasmasphere, and compute its contribution to the ring current for comparison with those of the solar, polar, and auroral winds. There have been some updates of our model of particularly the auroral wind outflow response to energy inputs, which reduce its contribution in comparison with the results of *Fok et al.* [2006]. The overall linkages of simulation modules is given in Figure 1.

3. Circulation Results

3.1. Solar, Polar, Auroral Winds

[13] We first summarize the results for solar wind, polar wind, and auroral wind behavior from our previous study [*Moore et al.*, 2007, Figures 3, 4, and 5]. There we reported on the computation of over 100 million solar wind proton trajectories, 1.5 million polar wind trajectories, and 3 million auroral wind trajectories, to study plasma circulation. The results illustrate many familiar features of magnetospheric plasma dynamics for this elementary substorm-like event. We emphasize here our earlier finding [*Moore et al.*, 2005] that solar wind entry occurs most prominently through the dawn flank for southward IMF conditions, and that an appreciable pressure of solar wind plasma arises in the inner magnetosphere.

[14] The initial state for northward IMF was derived from a few hours of steady conditions. The magnetotail is only about 30−40 R_E long, and the plasma sheet is so diffuse that it is undifferentiated from the polar lobes. High-latitude reconnection removes flux from the lobes and draws solar

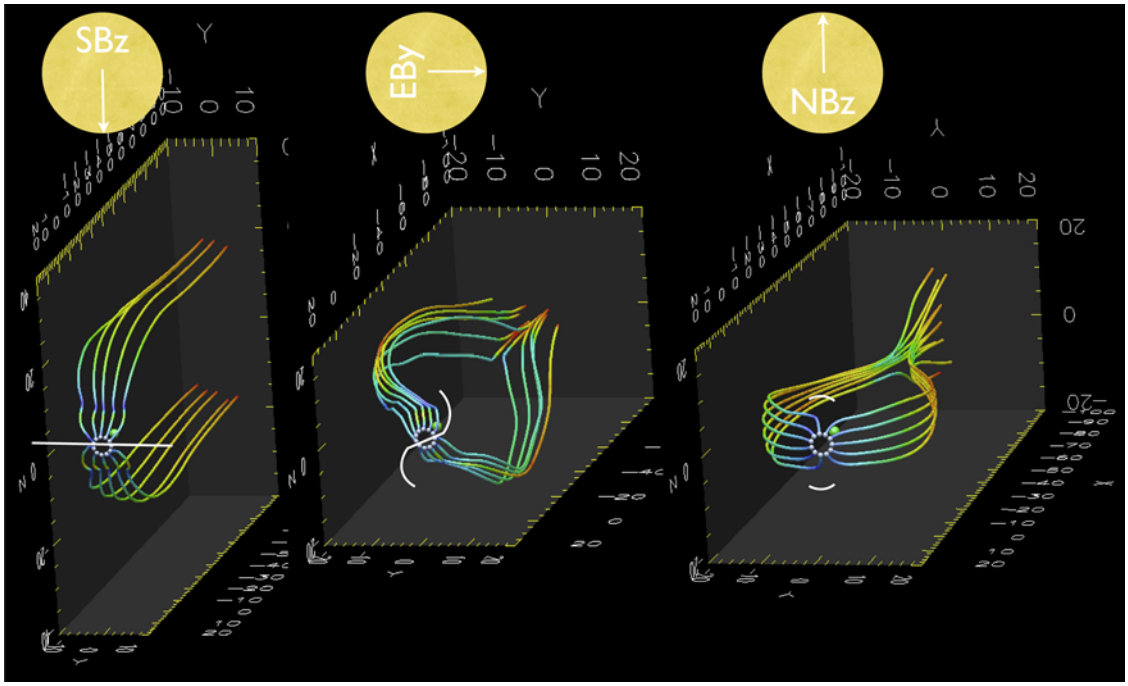

Figure 2. Configuration of dayside magnetosheath flow streamlines in the LFM global circulation model for northward, eastward, and southward IMF as indicated. Streamline speed is color-coded. The green dot is Earth, and the circle of silver dots marks the streamline starting points. The starting points are equally spaced around the x axis at a radius of 2 R_E at an X value as close as practical to the magnetopause (within the magnetosheath) so that these streamlines approach as close as practical to being tangential to the magnetopause.

plasma from the low-latitude boundary layers into the plasma sheet, up through the lobes, and then downstream. On the dayside, high-latitude reconnection produces freshly closed flux tubes that capture solar plasma and produce low-latitude boundary layer flux tubes that create cool dense plasmas and supply the above mentioned flows. Magnetosheath flow streamlines in the LMF simulation are illustrated in Figure 2, with Figure 2 (right) showing streamlines for northward IMF. The short white line segments denote the inferred regions of strong high-latitude reconnection along an estimated X line position. Figure 2 was produced from a long LFM run with steady northward IMF, to be sure that transient behaviors were cleared from the simulation. Polar wind outflow weightings were guided by observations [*Su et al.*, 1998], and produced realistic outflows into the lobes of low-density, low-energy outflows. A substantial amount of polar wind was found to enter the magnetosheath via high-latitude reconnection and to escape from the system downstream. Little auroral wind was found to be present at high altitudes in the magnetosphere during the initial northward B_z period.

[15] When southward IMF reaches the magnetosphere, it shifts reconnection to the subsolar equatorial region, as also illustrated in Figure 2 (left). This completely changes the magnetosheath flow, removing plasma and flux from the dayside magnetosphere and polar lobes, and after about 1 h initiates an episode of magnetotail reconnection and a substorm-like event with enhanced sunward convection and the ejection of a plasmoid. This substorm behavior has been the subject of a previous paper [*Fok et al.*, 1999] so it will not be discussed in detail here. However, simulations of that event show that the plasma injection produced at geosynchronous orbit is quite typical of the observed signatures of substorms. At this time, polar wind simulations produced realistic outflows into the lobes of low-density, low-energy outflows, while antisunward flow carried these protons to the region of the tail where reconnection was proceeding. Terminating this flow, a substantial amount of polar wind was found to enter the magnetosheath via low-latitude dayside reconnection and to escape from the system downstream, after flowing through the inner magnetosphere. Enhanced auroral wind was also driven by the enhanced auroral zone coupling of energy and solar wind plasmas. This auroral wind was much more confined to the inner magnetosphere than the polar wind protons, and a relatively small amount escaped into the dayside magnetosheath and downstream for this event.

3.2. Plasmaspheric Wind

[16] The first step in simulating the plasmaspheric wind was to establish a dynamic plasmasphere on the basis of the Ober model, as described above. The results of this are shown in Figure 3, at three times during the 3.5 h simulation period: early before the effects of southward IMF are significant; midway through the simulation while reconnection is driving strong convection, and late in the simulation after the IMF has turned northward, convection has subsided, and the plume is beginning to wrap owing to the effects of the ionosphere's rotation. These density values, evaluated at 6.6 R_E, are used to provide weightings

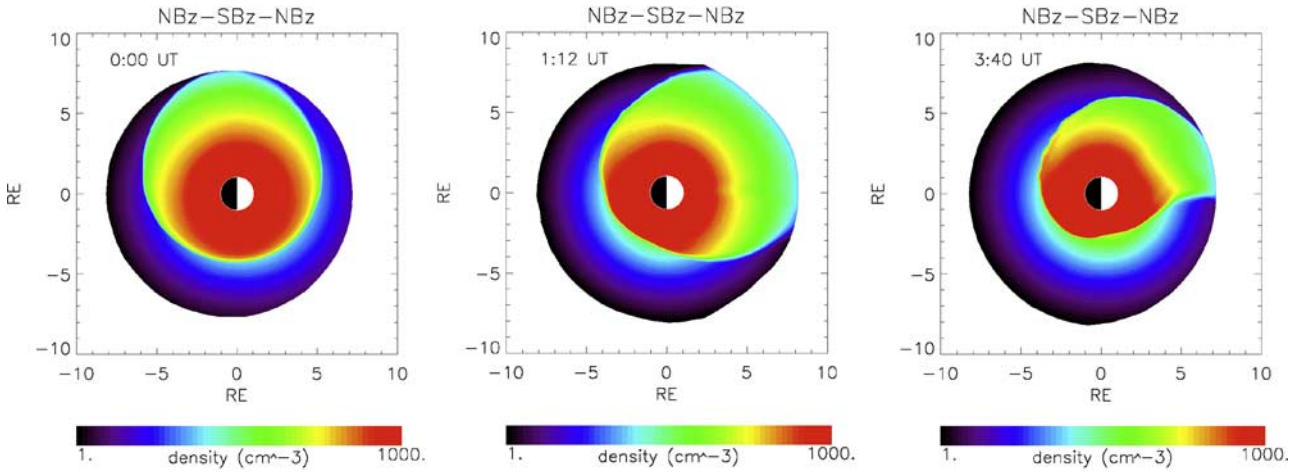

Figure 3. A plasmaspheric model derived from that of *Ober et al.* [1997] is used to generate plasma flux across the $L = 6.6$ shell as it responds to global convection driven by southward IMF. The simulation eventually exhibits wrapping by corotation when the IMF turns northward again and convection subsides.

of the protons whose motions are subsequently followed throughout the magnetosphere.

[17] The resultant plasmaspheric wind circulation is illustrated in Figure 4 at two times during the 3.5 h simulation sequence: at the beginning (Figure 4a) and midway through the simulation, when protons from the lobes are reaching the reconnecting plasma sheet. Initially, the only plasma shown is that of the cold quiescent plasmasphere. The IMF turns southward within 4 min of $T = 0$, and it takes about 30 min thereafter to draw the plasmaspheric plume leading edge (as individual test particles) out to the magnetopause. The peak density at the magnetopause is about 30 cm^{-3}. The protons then quickly disperse through the boundary layers and the polar cap region in the downstream direction. In about an additional hour, they have reached the plasma sheet, where reconnection had begun about a half hour earlier. Magnetotail reconnection bifurcates the flow into tailward and sunward components, the latter of which occurs in two nearly symmetric flow channels. The plasmasphere has by that time assumed the characteristic active configuration with a sharpened gradient through the midnight sector and a plume extending directly toward the sun with some asymmetry toward the afternoon sector.

[18] The IMF turns northward again after about 2 h, shutting down the inner magnetospheric circulation and seeking to reestablish the initial state of the magnetosphere for this simulation. 1.5 h is insufficient to fully complete this process, but the formation of high-latitude reconnection sites and the evacuation of the lobes is apparent in the sequence of Figure 8. By the end of the simulation, the plasmasphere is expanding steadily in Z_{GSM} into the lobes. The duration of this simulation is sufficient to produce only a slight bit of wrapping of the plume by inner magnetosphere corotation.

4. Global Impact Results

[19] We first look at the aggregate supply of plasma ions to the inner magnetosphere, from the four sources: solar wind, polar wind, auroral wind, and now plasmaspheric

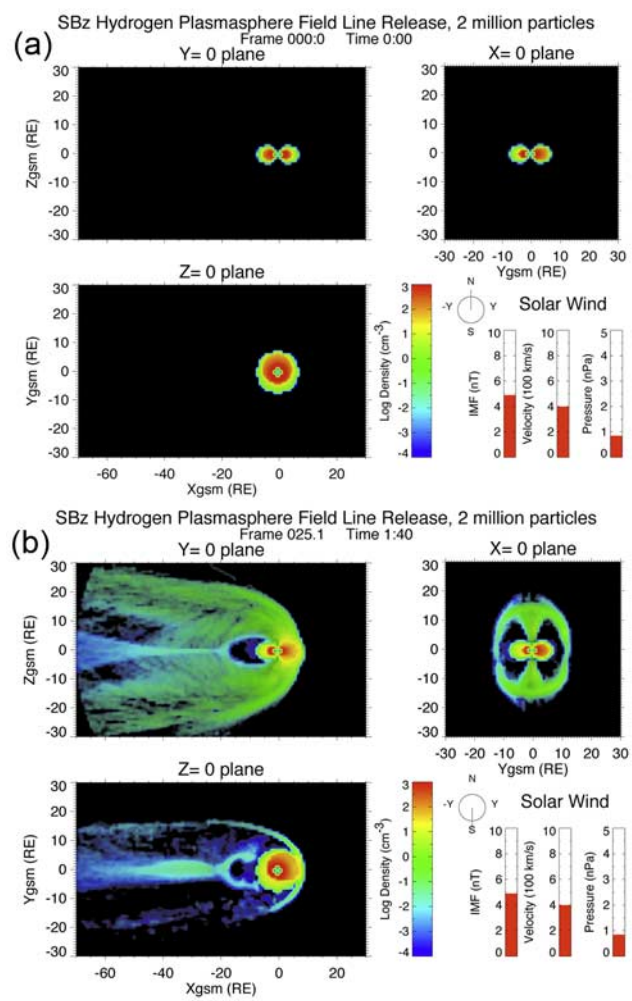

Figure 4. (a) The plasmaspheric wind initial conditions (00:00 h), and the response to southward IMF, with (b) resultant day and night side reconnection (01:40 h).

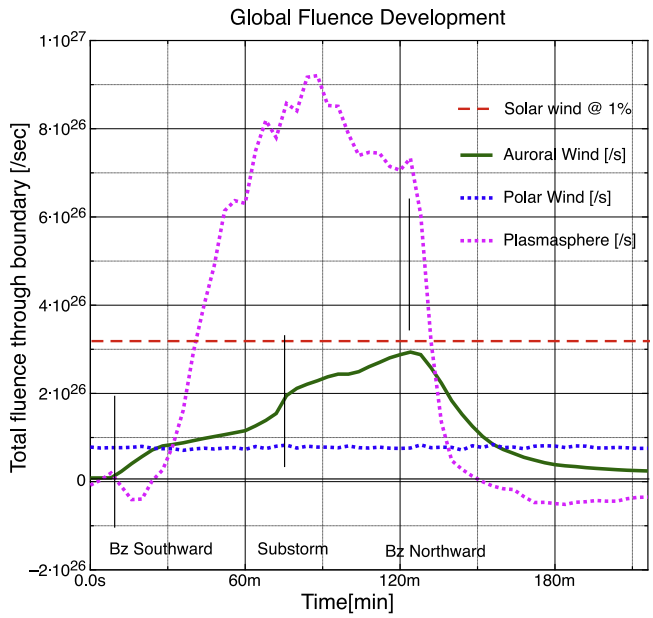

Figure 5. The total fluence of ions into the magnetosphere for this event is compared for solar wind (nominal 1%), polar wind, auroral wind, and plasmaspheric wind, as indicated.

wind. The result is given in Figure 5, where we see that the plasmaspheric wind is certainly the most responsive to this simulation sequence. This is as expected, since in quiet times, there should be negligible escape of plasma from the plasmasphere. For this event, the fluence rises steeply with onset of convection to a peak of nearly 10^{27} ions/sec and then subsides when convection is turned off by arrival of northward IMF. Though we have not computed it, we should expect that the application of persistent southward IMF would lead to a subsidence of the efflux in the plasmaspheric plasma to a value commensurate with the polar wind flux integrated over the area of the ionosphere below approximately 55° latitude, that is, within the plasmasphere proper. The large fluence seen in this event is purely transient in nature, owing to the release of a substantial volume of high-density plasma that has built up from relatively low fluxes over a substantial period.

[20] The polar wind fluence here, as shown on the plot, is a fixed value just below 10^{26} proton/s, when integrated over the regions above 55° latitude, on the basis of observed peak fluxes and solar zenith angle dependences [*Su et al.*, 1998]. There is no influence of the solar wind interaction on the fluence, only upon the circulation and escape of these plasmas.

[21] The auroral wind fluence is strongly influenced by the energy inputs to the ionosphere owing to the changing IMF and enhanced solar wind interaction in the auroral zone, as discussed in detail by *Moore et al.* [2007]. For this event the fluence increases with a jump upward in response to the onset of tail reconnection, to a peak of $\sim 3 \times 10^{26}$ O^+/s prior to the northward turning of IMF.

[22] The value shown for solar wind entry into the inner magnetosphere is based on a simple scaling of the solar wind flux incident upon the magnetosphere and a somewhat arbitrary assumption of 1% entry. Though we have solar wind proton trajectories that could be used to better evaluate this number, it is strongly dependent upon the definition of the "inner magnetosphere" and we have yet to devise a method that seems satisfactory. Most of the solar wind continues past the magnetosphere, but a substantial amount of it enters inside the magnetopause without entering the main closed cell circulation within the magnetosphere. The fraction that does indeed enter closed interior circulation is what is so difficult to determine. However, we have evaluated the amount of solar wind plasma in the inner magnetosphere and its variations, as shown below.

[23] Next we examine the total plasma content of the inner magnetosphere, defined as the region inside the CRCM simulation boundary at $L = 8$. The result of integrating total particle content over this volume is shown in Figure 6. Here we see that the SB_z period has significantly eroded the plasmaspheric content, with about 60% of it being removed by this short period of enhanced convection. Similarly, the polar wind content of the inner region is reduced owing to the same kind of losses into the boundary layers that erode the plasmasphere rather than simply circulating it. An increase in solar wind content inside the inner magnetosphere clearly results, amounting to about one third of the loss of plasmaspheric ions or one fifth of the initial plasmaspheric content. A smaller though comparable increase in the auroral wind (O^+) content also occurs, albeit with a delay of about 1 h. Perhaps the most significant point here, and the most counterintuitive, is that lighter ionospheric species are mainly lost from the inner magnetosphere owing to enhanced magnetospheric circulation, the losses occurring as these light and relatively fast ions escape into the boundary layers and magnetosheath.

[24] We can also now compare the ring current contributions of all four sources in this simulation: solar wind, polar

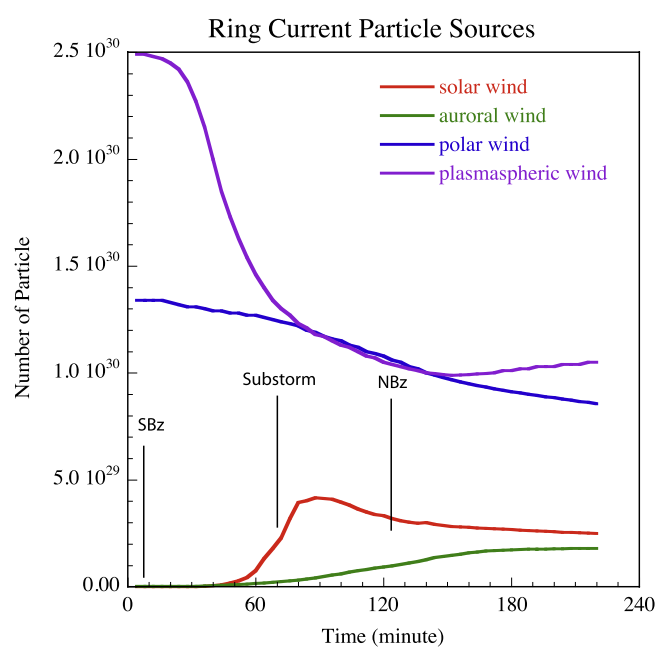

Figure 6. Inner magnetosphere plasma particle content development during the simulation for the four sources considered, integrating over the domain of the CRCM simulation inside of $L = 8$.

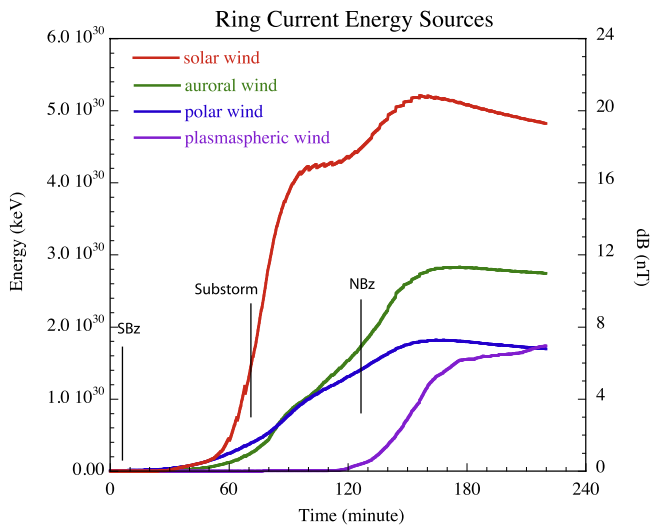

Figure 7. Inner magnetosphere kinetic energy content development during the simulation for the four sources considered, integrating over the domain of the CRCM simulation inside of $L = 8$.

wind, auroral wind, and now plasmaspheric wind. Figure 7 summarizes this comparison, showing that the bulk of ring current generation for this event originates with solar wind protons entering the inner magnetosphere as previously reported [*Moore et al.*, 2005]. The next largest contributor to the ring current for this event is the auroral wind of escaping O^+. The smallest contributions, which are of comparable size, come from the polar wind and from the plasmaspheric wind. The former is relatively prompt owing to its continuous presence in the magnetospheric lobes and magnetotail, while the latter is somewhat delayed from its initial transient release by transport time from the plasmasphere through the plasma sheet and back to the inner magnetosphere after energization.

5. Discussion

[25] We have shown here that a large fluence of low-energy protons will be released by a typical enhancement of magnetospheric convection associated with an isolated substorm. The simulated transient fluence exceeds the normal polar wind outflow by 1 order of magnitude and also exceeds the amount of auroral wind O^+ released in the simulated event we studied here. This is as expected and no great surprise to those who have been studying the appearance of low-energy convecting plasmas in the outer magnetosphere. The time series results appear in Figures 6 and 7. Comparison of Figures 6 and 7 shows that the mean energy of the plasmaspheric ions inside the CRCM part of the simulation rises from an initial value of about 1 eV to greater than 1 keV, considering both the remaining cold core and the component that has been accelerated during circulation. The plasmaspheric simulation is continually supplying more cold protons, while the energetic protons will be lost by precipitation and charge exchange. The combination of these processes will lead to a decay of both the total energy and the mean energy in the plasmasphere. An overview of the full temporal development is given in Figure 8, using selected frames of the plasmaspheric proton pressure distribution, from the current simulation. The frames illustrate the initial confinement of the plasmasphere to its normal domain, the effect of the onset of dayside low-latitude reconnection when the IMF turns southward, then the onset of nightside reconnection, and finally, the onset of high-latitude reconnection when the IMF turns northward again, and the initial stages of return toward the initial state. The unexpected aspect of this study lies in the fact that so large a fluence of ionospheric plasma into the magnetosphere produces a relatively small contribution to the ring current plasma energy. It is no larger than the contribution of polar wind, despite the fact that the escaping fluence is 1 order of magnitude larger. We conclude from this that, at least for substorm-scale events, the plasmaspheric wind plasmas are for the most part released entirely from the magnetosphere into the boundary layers, the magnetosheath, and solar wind flow downstream, rather than being recycled through the inner plasma sheet and inner magnetospheric energization processes. Since so much plasma is released into the magnetosheath, it may be that it has observable features in that medium. For example, one may anticipate locally enhanced density, or enhanced He^+ composition relative to the surrounding solar wind. Any such features may be expected downstream of reconnection features on the dayside magnetopause.

[26] Following *Delcourt et al.* [1992], we may also inquire as to how the cold plasmaspheric wind plasma behaves kinetically in the outer cusp region. That investigation found that capture and entry of solar wind protons into the inner magnetosphere was influenced by trapping and nonadiabatic energization in the cusp field strength minimum. The same effects should be studied now with plasmaspheric plasma properties as the assumed boundary condition. However, investigation of the thermalization of energy gained from pickup on solar wind-connected flux tubes, while certainly possible, is beyond the scope of the present paper.

[27] Another unexpected aspect of this work is that the density of the plume plasma drops precipitously as it passes through the dayside reconnection and cusp regions, such that plasmaspheric values of density are not seen in the polar lobe regions, contrary to the suggestion of *Elphic et al.* [1997] and *Borovsky et al.* [1997]. This is in large part a consequence of the rapid expansion of flux tubes in this region, especially as they pass into the polar lobes. Another contributing factor is certainly the energization of cold protons that suddenly find themselves on rapidly moving flux tubes powered by conjugate solar wind plasmas.

[28] We infer that the initial energy of plasma ions in the magnetospheric system seems to be irrelevant to their ultimate fate. Of the fast and light protons, only a small fraction will be circulated into the interior magnetosphere. The bulk of them will be picked up by the solar wind to like velocities and escape downstream as soon as they convect onto open or boundary layer flux tubes. On the other hand, most of the slow and heavy O^+ ions will remain relatively close to the Earth and escape into the magnetosheath to a lesser degree, and at higher energy. They will tend to make multiple trips around the magnetospheric circulation path, gaining energy until they are finally fast enough to behave like protons and escape into the magnetosheath. Thus, while

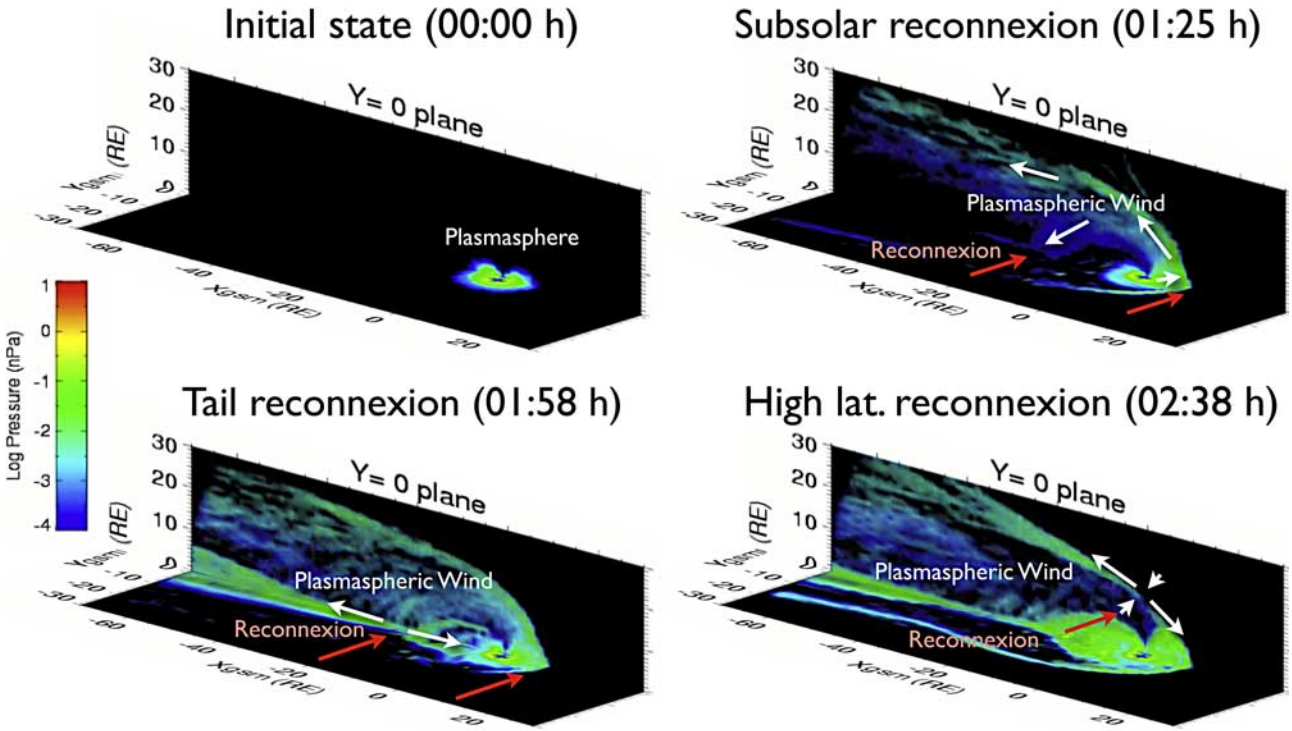

Figure 8. A comparison of plasmaspheric pressure distributions, as indicated by the color bar at the right, in two orthogonal slices through the simulation space at four times during the simulation, as indicated.

trapping by gravity ceases as soon as O^+ ions are accelerated above 10 eV, their large mass and slow velocity at given energy remains a significant factor in retaining them close to Earth. Conversely, geogenic protons reach the magnetosheath more readily, mixing with solar protons there.

6. Conclusions

[29] On the basis of our simulations of the full trajectories of solar and ionospheric ions in 3-D magnetospheric fields from a global simulation, we conclude the following:

[30] Plasmaspheric plumes should indeed produce densities of several 10 s cm^{-3} inside the dayside magnetospheric boundary layers, exceeding the polar wind efflux by 1 order of magnitude for even modest enhancements of magnetospheric convection associated with isolated substorms.

[31] Because such plasmaspheric plumes are associated with the release of pent up polar wind outflows that have been trapped in the equatorial region, we propose the name of "plasmaspheric wind" for their circulation throughout the magnetosphere.

[32] On the basis of the motion of plume particles in 3-D global fields, we conclude that the bulk of the plasmaspheric wind will escape from the magnetosphere downstream, rather than being recycled through the inner magnetosphere, so its contribution to energetic storm time plasmas is comparable with that of the polar wind.

[33] In contrast, solar wind entry is enhanced during the simulated period of southward IMF and strong coupling with the magnetosphere, so that it contributes the dominant increment of the resulting ring current.

[34] These results must be qualified by the knowledge that we have considered only test particles in MHD fields that are consistent with negligible presence of ionospheric species. The exception is that within the CRCM inner magnetospheric simulation, ionospheric plasmas are dynamic elements that do alter the global convection pattern. However, these results could change, perhaps significantly, and will be superceded by multifluid studies that compute the influence of ionospheric plasma inertia and pressure in the outer magnetosphere.

[35] **Acknowledgments.** We thank Dan Ober for access to his plasmaspheric simulation code, and Robert Strangeway for his unpublished parameterization of O^+ outflow temperature response to incident Poynting flux. We also thank Manuel Buenfil, whose mathematics, programming, database, and visualization mastery made this work possible. We acknowledge support from the NASA Heliophysics Division through the ROSES program under WBS 370544.01.01, the NASA Polar Mission under WBS 889836.04.05, and NASA's High Performance Computing Program under task R0608.

[36] Zuyin Pu thanks Joseph Borovsky and another reviewer for their assistance in evaluating this manuscript.

References

Borovsky, J. E., and M. H. Denton (2006), Effect of plasmaspheric drainage plumes on solar-wind/magnetosphere coupling, *Geophys. Res. Lett.*, *33*(20), L20101, doi:10.1029/2006GL026519.

Borovsky, J. E., M. F. Thomsen, and D. J. McComas (1997), The superdense plasma sheet: Plasmaspheric origin, solar wind origin, or ionospheric origin?, *J. Geophys. Res.*, *102*, 22,089.

Chandler, M. O., and T. E. Moore (2003), Observations of the geopause at the equatorial magnetopause: Density and temperature, *Geophys. Res. Lett.*, *30*(16), 1869, doi:10.1029/2003GL017611.

Chappell, C. R., K. K. Harris, and G. W. Sharp (1970), A study of the influence of magnetic activity on the location of the plasmapause as measured by OGO 5, *J. Geophys. Res.*, *75*, 50, doi:10.1029/JA075i001p00050.

Chappell, C. R., K. K. Harris, and G. W. Sharp (1971), The dayside of the plasmasphere, *J. Geophys. Res.*, *76*, 7632, doi:10.1029/JA076i031p07632.

Chen, S.-H., and T. E. Moore (2004), Dayside flow bursts in the Earth's outer magnetosphere, *J. Geophys. Res.*, *109*, A03215, doi:10.1029/2003JA010007.

Chen, S.-H., and T. E. Moore (2006), Magnetospheric convection and thermal ions in the dayside outer magnetosphere, *J. Geophys. Res.*, *111*, A03215, doi:10.1029/2005JA011084.

Delcourt, D. C., T. E. Moore, J. A. Sauvaud, and C. R. Chappell (1992), Nonadiabatic transport features in the outer cusp region, *J. Geophys. Res.*, *97*(A11), 16,833, doi:10.1029/92JA00834.

Delcourt, D. C., J. A. Sauvaud, and T. E. Moore (1993), Polar wind ion dynamics in the magnetotail, *J. Geophys. Res.*, *98*(A6), 9155, doi:10.1029/93JA00301.

Elphic, R. C., M. F. Thomsen, and J. E. Borovsky (1997), The fate of the outer plasmasphere, *Geophys. Res. Lett.*, *24*(4), 365, doi:10.1029/97GL00141.

Fok, M.-C., T. E. Moore, and D. C. Delcourt (1999), Storm time modeling of the inner plasma sheet/outer ring current, *J. Geophys. Res.*, *104*(A7), 14,557, doi:10.1029/1999JA900014.

Fok, M.-C., R. A. Wolf, R. W. Spiro, and T. E. Moore (2001), Comprehensive computational model of Earth's ring current, *J. Geophys. Res.*, *106*(A5), 8417.

Fok, M.-C., T. E. Moore, P. C. Brandt, D. C. Delcourt, S. P. Slinker, and J. A. Fedder (2006), Impulsive enhancements of oxygen ions during substorms, *J. Geophys. Res.*, *111*, A10222, doi:10.1029/2006JA011839.

Foster, J. C., A. J. Coster, P. J. Erickson, F. J. Rich, and B. R. Sandel (2004), Stormtime observations of the flux of plasmaspheric ions to the dayside cusp/magnetopause, *Geophys. Res. Lett.*, *31*, L08809, doi:10.1029/2004GL020082.

Freeman, J. W., H. K. Hills, T. W. Hill, P. H. Reiff, and D. A. Hardy (1977), Heavy ion circulation in the Earth's magnetosphere, *Geophys. Res. Lett.*, *4*, 195, doi:10.1029/GL004i005p00195.

Goldstein, J., B. R. Sandel, M. F. Thomsen, M. Spasojević, and P. H. Reiff (2004), Simultaneous remote sensing and in situ observations of plasmaspheric drainage plumes, *J. Geophys. Res.*, *109*, A03202, doi:10.1029/2003JA010281.

Grebowsky, J. M. (1970), Model study of plasmapause motion, *J. Geophys. Res.*, *75*, 4329.

Lyon, J. G., J. A. Fedder, and C. M. Mobarry (2004), The Lyon-Fedder-Mobarry (LFM) global MHD magnetospheric simulation code, *J. Atmos. Sol. Terr. Phys.*, *66*(15–16), 1333, doi:10.1016/j.jastp.2004.03.020.

Moore, T. E., et al. (2005), Plasma sheet and ring current formation from solar and polar wind sources, *J. Geophys. Res.*, *110*, A02210, doi:10.1029/2004JA010563.

Moore, T. E., M.-C. Fok, D. C. Delcourt, S. P. Slinker, and J. A. Fedder (2007), Global aspects of solar wind–ionosphere interactions, *J. Atmos. Sol. Terr. Phys.*, *69*, 265, doi:10.1016/j.jastp.2006.08.009.

Ober, D. M., J. L. Horwitz, and D. L. Gallagher (1997), Formation of density troughs embedded in the outer plasmasphere by subauroral ion drift events, *J. Geophys. Res.*, *102*, 14,595, doi:10.1029/97JA01046.

Peroomian, V., M. El-Alaoui, M. A. Abdalla, and L. M. Zelenyi (2007), A comparison of solar wind and ionospheric plasma contributions to the September 24–25, 1998 magnetic storm, *J. Atmos. Sol. Terr. Phys.*, *69*, 212–222, doi:10.1016/j.jastp.2006.07.025.

Sandel, B. R., et al. (2001), Initial results from the IMAGE extreme ultraviolet imager, *Geophys. Res. Lett.*, *28*(8), 1439.

Slinker, S. P., et al. (1999), Comparisons of global MHD simulations with AMIE simulations for the events of May 19–20, 1996, *J. Geophys. Res.*, *104*, 28,379, doi:10.1029/1999JA900403.

Su, Y.-J., et al. (1998), Polar wind survey with TIDE/PSI suite abroad POLAR, *J. Geophys. Res.*, *103*, 29,305, doi:10.1029/98JA02662.

Su, Y.-J., J. E. Borovsky, M. F. Thomsen, N. Dubouloz, M. O. Chandler, T. E. Moore, and M. Bouhram (2001a), Plasmaspheric material on high-latitude open field lines, *J. Geophys. Res.*, *106*(A4), 6085.

Su, Y.-J., M. F. Thomsen, J. E. Borovsky, and J. C. Foster (2001b), A linkage between polar patches and plasmaspheric drainage plumes, *Geophys. Res. Lett.*, *28*, 111, doi:10.1029/2000GL012042.

D. C. Delcourt, Centre d'Études des l'Environnements Terrestre et Planétaires, UMR 8639, 4 Avenue de Neptune, Saint-Maur des Fossés, F-94107, France.

J. A. Fedder, Icarus Research Inc., 7113 Exfair Road, Bethesda, MD 20814, USA.

M.-C. Fok and T. E. Moore, NASA Goddard Space Flight Center, 8800 Greenbelt Road, Code 670, Greenbelt, MD 20771, USA. (thomas.e.moore@nasa.gov)

S. P. Slinker, Naval Research Laboratory, 4555 Overlook Avenue SW, Washington, DC 20375, USA.